
Modeling Winner-Take-All Competition in Sparse Binary Projections

Wenye Li

School of Science and Engineering
The Chinese University of Hong Kong, Shenzhen
Shenzhen, Guangdong, China
wyl@cuhk.edu.cn

Abstract

Inspired by the advances in biological science, the study of sparse binary projection models has attracted considerable recent research attention. The models project dense input samples into a higher-dimensional space and output sparse binary vectors after Winner-Take-All competition, subject to the constraint that the projection matrix is also sparse and binary. Following the work along this line, we developed a supervised-WTA model under the supervised setting where training samples with both input and output representations are available, from which the projection matrix can be obtained with a simple, efficient yet effective algorithm. We further extended the model and the algorithm to an unsupervised setting where only the input representation of the samples is available. In a series of empirical evaluation on similarity search tasks, both models reported significantly improved results over the state-of-the-art methods in both search accuracy and running time. The successful results give us strong confidence that the proposed work provides a highly practical tool to real world applications.

1 Introduction

Random projection has emerged as a powerful tool in data analysis applications [3]. It is often used to reduce the dimension of a set of data samples in the Euclidean space. It provides a simple and computationally efficient way to reduce the storage complexity of the data by trading a controlled amount of representation error for faster processing speed and smaller model sizes [13].

Very recently, with strong biological evidence, a sparse binary projection model called the FLY algorithm was designed and attracted people's much attention. Instead of performing dimension reduction, the algorithm increases the dimension of the input samples with a random sparse binary projection matrix. After winner-take-all (WTA) competition in the output space, the samples are converted into a set of sparse binary vectors. In similarity search tasks, it was reported that such sparse binary vectors outperformed the hashed vectors produced by the classical locality sensitive hashing (LSH) method that is based on the conventional random projection [6].

Following the work along this line, we proposed two models with the explicit modeling of the WTA competition. Instead of residing on the random generation of the projection matrix, one of our models seeks the projection matrix under a supervised setting, while the other model operates purely in an unsupervised manner. For each model, we derived an algorithm that is surprisingly simple, yet with significantly improved empirical results in both similarity search accuracy and running speed over the state-of-the-art approaches.

A note on notation. Unless specified otherwise, a capital letter, such as W , denotes a matrix. A lower-cased letter, with or without a subscript, denotes a vector or a scalar. For example w_i denotes the i -th row, $w_{.j}$ denotes the j -th column, and w_{ij} denotes the (i, j) -th entry of the matrix W .

2 Background

2.1 Sparse Binary Projection Algorithms

Different from classical projection methods that commonly map data from a higher-dimensional space to a lower-dimensional space, the FLY algorithm increases the dimension of the data. It was designed by simulating the fruit fly’s olfactory circuit, whose function is to associate similar odors with similar tags. For a fly to process, each odor is initially represented as a 50-dimensional feature vector of firing rates. To associate each odor with a tag involves three steps. The first step is a divisive normalization step [19], which centers the mean of the feature vector. The second step expands the dimension of the feature vector from 50 to 2,000 with a sparse binary connection matrix [4, 26], which has the same number of ones in each row. The third step involves WTA competition as a result of strong inhibitory feedback coming from an inhibitory neuron. After the competition, all but the highest-firing 5% out of the 2,000 features are silenced [24]. These remaining 5% features just correspond to the tag assigned to the input odor.

The FLY algorithm can be regarded as a special form of the locality sensitive hashing (LSH) method which produces similar hashes for similar input samples. But different from the LSH method which reduces the data dimension, the FLY algorithm increases the dimension with a random sparse binary matrix, while ensuring the sparsity and binarization of the data in the output space. Empirically, the FLY algorithm reported improved results over the LSH method [6] in similarity search applications.

The success of the FLY algorithm inspired considerable research attention, among which one of particular interest to us is the LIFTING algorithm [16] that removes the randomness assumption of the projection matrix, which is partially supported by most recent biological discoveries [26]. In the work, the projection matrix is obtained through supervised learning. Suppose training samples with both dense input representation $X \in \mathcal{R}^{d \times m}$ and sparse output representation $Y \in \{0, 1\}^{d' \times m}$ are available. The LIFTING algorithm seeks the projection matrix W that minimizes $\|WX - Y\|_F^2 + \beta \|W\|_{\frac{1}{2}}$ in the feasible region of sparse binary matrices. To solve the optimization problem, the Frank-Wolfe algorithm [7, 10] can be applied with quite good performance.

2.2 Winner-Take-All Competition

Evidences in neuroscience showed that excitation and inhibition are common activities in neurons [24, 25]. Based on the lateral information, some neurons raise to the excitatory state; while the rest get inhibited and remain silent. The excitation and inhibition result in the competition among neurons. Modeling such neuron competitions is of key importance. Computational models that involve the competition stage are found in wide applications, such as in computational brain models, artificial neural networks and analog circuits design [1, 18]. In machine learning, the competition mechanism has motivated the design of computer algorithms for a long time, from the early self-organizing map [14] to more recent work in developing novel neural network architectures [21, 17].

To model the competition stage, the WTA model is routinely adopted. We are interested with a variant of the WTA model with the following form. For a d -dimensional input vector x and a given hash length k ($k \ll d$), the WTA competition computes a function $WTA_k^d : \mathcal{R}^d \rightarrow \{0, 1\}^d$ with the output $y = WTA_k^d(x)$ satisfying, for each $1 \leq i \leq d$,

$$y_i = \begin{cases} 1, & \text{if } x_i \text{ is among the } k\text{-largest entries of } (x_1, \dots, x_d). \\ 0, & \text{otherwise.} \end{cases} \quad (1)$$

Thus the output entries with value 1 just mark the positions of the k -largest values of x . For simplicity and without causing ambiguity, we will not differentiate whether the input/output vector of the WTA function is a row vector or a column vector.

3 Model

3.1 Supervised Training

Let a set of samples be in the form of $X \in \mathcal{R}^{d \times n}$ and $Y \in \{0, 1\}^{d' \times n}$ with each $x_{.m}$ ($1 \leq m \leq n$) being an input sample and $y_{.m}$ being its output representation satisfying $\|y_{.m}\|_1 = k$ for a given k . We assume that there exists a projection matrix $W \in \{0, 1\}^{d' \times d}$ with each $\|w_{i.}\|_1 = c$ ($1 \leq i \leq d'$) for a given c ¹, such that each $y_{.m} = WT A_k^{d'} (Wx_{.m})$ holds.

From the definition of the WTA function in Eq. (1), in addition to the sparse and binary constraints, a necessary and sufficient condition for the projection matrix W is:

$$w_{i.}x_{.m} \geq w_{j.}x_{.m}, \text{ if } y_{im} = 1 \text{ and } y_{jm} = 0 \quad (2)$$

for all $1 \leq m \leq n$ and $1 \leq i, j \leq d'$.

In a supervised setting, we are interested in finding such a projection matrix W with given X and Y . But unfortunately, solving the problem directly from Eq. (2) is generally hard. A matrix that satisfies all the constraints may not exist at all for real data. Even if it exists, the computational requirement can be non-trivial. A straightforward approach, modeling the problem as a linear integer program, would involve $d' \times d$ variables and $O(nk(d' - k) + d')$ constraints, which is infeasible to solve even for moderately small n and d' .

To handle the difficulty, the problem can be relaxed. For each i, j and m , define a measure $y_{im}(1 - y_{jm})(w_{i.}x_{.m} - w_{j.}x_{.m})$ to quantify the compliance with the condition in Eq. (2). If $y_{im} = 1$ and $y_{jm} = 0$, its value is non-negative when the condition is met; otherwise, it is negative. Naturally, we sum up the measure over all possible m, i, j , and have

$$L_s(W) = \sum_{m=1}^n \sum_{i=1}^{d'} \sum_{j=1}^{d'} y_{im}(1 - y_{jm})(w_{i.}x_{.m} - w_{j.}x_{.m}). \quad (3)$$

The value of $L_s(W)$ measures how well a matrix W meets the conditions in Eq. (2). Therefore maximizing L_s with respect to W in the feasible region of sparse binary matrices provides a principled solution to finding the projection matrix. And we call this the supervised-WTA model.

From an algorithmic viewpoint, maximizing $L_s(W)$ is equivalent to d' maximization sub-problems. Each sub-problem seeks a row vector $w_{i.}$ ($1 \leq i \leq d'$) by

$$\max w_{i.} \left[\sum_{m=1}^n x_{.m} \left(y_{im} - \frac{k}{d'} \right) \right] \quad (4)$$

subject to:

$$w_{i.} \in \{0, 1\}^{1 \times d}, \text{ and } \|w_{i.}\|_1 = c. \quad (5)$$

Let

$$\ell_{.i} = \sum_{m=1}^n x_{.m} \left(y_{im} - \frac{k}{d'} \right), \quad (6)$$

and the optimal solution of $w_{i.}$ to Eq. (4) is given by

$$w_{i.}^* = WTA_c^d(\ell_{.i}) \quad (7)$$

3.2 Unsupervised Training

The supervised-WTA model utilizes both input and output representations to learn a projection matrix. When only the input representation is available, we can extend the work to an unsupervised-WTA model, by maximizing the objective:

$$L_u(W, Y) = \sum_{m=1}^n \sum_{i=1}^{d'} \sum_{j=1}^{d'} y_{im}(1 - y_{jm})(w_{i.}x_{.m} - w_{j.}x_{.m}) \quad (8)$$

¹Following the work of [6], c is set to $\lfloor 0.1 \times d \rfloor$ in this paper.

satisfying

$$w_{i.} \in \{0, 1\}^{1 \times d}, \|w_{i.}\|_1 = c, y_{.m} \in \{0, 1\}^{d' \times 1}, \text{ and } \|y_{.m}\|_1 = k \quad (9)$$

for all $1 \leq i \leq d'$ and $1 \leq m \leq n$.

Different from the supervised-WTA model, the unsupervised model treats the unknown output representation Y as a variable, and jointly optimizes on both W and Y . To maximize L_u , an alternating algorithm can be used. Start with a random initialization of W as W^1 , and solve the model iteratively. In t -th ($t = 1, 2, \dots$) iteration, maximize $L_u(W^t, Y)$ with respect to Y and get the optimal Y^t . Then maximize $L_u(W, Y^t)$ with respect to W and get the optimal W^{t+1} .

The optimal Y^t is given by:

$$y_{.m}^t = W T A_k^{d'} (W^t x_{.m}) \quad (10)$$

for all $1 \leq m \leq n$. Similarly to the supervised setting, the optimal W^{t+1} is given by:

$$w_{i.}^{t+1} = W T A_c^d (\ell_{.i}^t) \quad (11)$$

for all $1 \leq i \leq d'$, where $\ell_{.i}^t = \sum_{m=1}^n x_{.m} (y_{im}^t - \frac{k}{d'})$.

Denote by $L_u^t = L_u(W^t, Y^t)$. Obviously, the sequence $\{L_u^t\}$ monotonically increases for $t = 1, 2, \dots$. Therefore the alternating optimization process is guaranteed to converge when the objective value L_u^t can't be increased any more.

It is worth mentioning that the unsupervised-WTA model can be studied as a clustering method [11]. The model puts m data samples into d' clusters and each sample belongs to k clusters. A special case of $k = 1$ corresponds to a hard clustering method. Two samples with the element of one in the same output dimension means they belong to the same cluster. Due to the existence of the clustering effects, the model is able to put semantically related language words into the same group in an experiment with word vectors, as reported in Section 4.3.

The unsupervised-WTA model can also be treated as a feature selection method [9]. This can be seen from the fact that each output dimension is associated with a subset of c features only, instead of all d features in the input space. The model is able to choose these c features automatically and encode the information in the projection matrix W . A detailed discussion of the clustering and the feature selection viewpoints goes beyond the scope of this paper and is hence omitted.

3.3 Complexity Issues

Solving the supervised-WTA model is computationally straightforward and can be implemented with high efficiency. For each projection vector $w_{i.}$, a naïve implementation needs $O(dm + d \log c)$ operations, among which $O(dm)$ are for the summation operation in Eq. (6) and $O(d \log c)$ are for the sorting operations in Eq. (7). Therefore, computing the whole projection matrix needs $O(d'dm + d'd \log c)$ operations. In fact, by utilizing the sparse structure of the output matrix Y , the computational complexity for W can be further reduced to $O(kdm + d'd \log c)$. As seen in Section 4.4, this is a highly efficient result.

To solve the unsupervised-WTA model, each iteration we need to compute both Y and W . Solving one Y needs $O(cdm + d'd \log k)$ operations by utilizing the sparse structure of W , where $O(cdm)$ are for multiplying W with X and $O(d'd \log k)$ are for the sorting operations in Eq. (10). Computing one W has the same complexity as in the supervised-WTA model, $O(kdm + d'd \log c)$. Therefore, the total complexity per iteration is $O((k+c)dm + d'd \log(kc))$, which is also an efficient solution as seen in Section 4.4.

For both supervised-WTA and unsupervised-WTA models, the memory requirement comes mainly from the matrices X , Y and W , and the storage complexity is $O(dm + d'm + d'd)$, which can be further reduced to $O(dm + km + d'c)$ if sparse matrix representation is used.

Both training algorithms are parallelizable. Each vector of W and Y can be solved independently with high parallel efficiency. It is also notable that, through simple pre-processing of the training data, all the computations in the algorithms will only involve simple vector addition and scalar comparison operations, which can often be a useful property in practice.

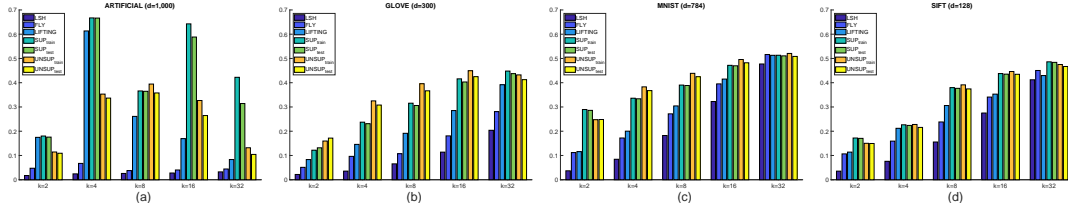


Figure 1: **Comparison of similarity search accuracies on different datasets** ($d' = 2,000$). The horizontal axis is the hash length ($k = 2/4/8/16/32$). The vertical axis is the search accuracy. (For better visualization effect of the results shown in color, the reader is referred to the soft copy of this paper.)

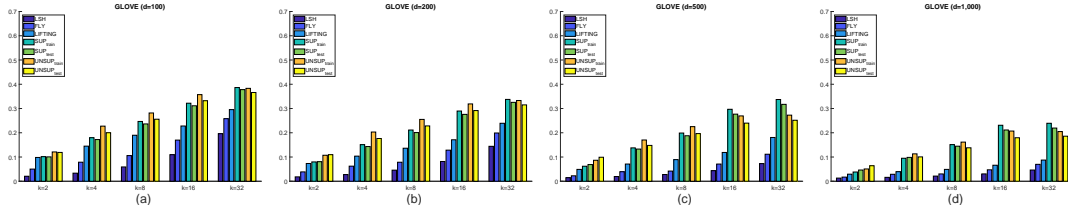


Figure 2: **Comparison of similarity search accuracies on GLOVE dataset with different input dimensions and fixed output dimension** ($d = 100/200/500/1,000$, $d' = 2,000$). The horizontal axis is the hash length ($k = 2/4/8/16/32$). The vertical axis is the search accuracy. (For better visualization effect of the results shown in color, the reader is referred to the soft copy of this paper.)

4 Evaluation

4.1 General Settings

To evaluate the performance of the proposed models, we carried out a series of experiments under the following settings.

Application: Similarly to the work of [6], we applied the proposed models in similarity search applications. Similarity search aims to find similar samples to a given query object among potential candidates, according to a certain distance or similarity measure [2]. The complexity of accurately determining similar samples relies heavily on both the number of candidates and their dimension. Computing the distances seems straightforward, but unfortunately could often become prohibitive if the number of candidates is too large or the dimension of the data is too high.

To handle the difficulty brought by the high dimension of the input data, we can either reduce the data dimension while approximately preserving their pairwise distances, or increase the dimension but confining the data in the output space to be sparse and binary, in the hope of significantly improved search speed with the new representation.

Objective: Our major objective is to evaluate and compare the similarity search accuracies for different algorithms. Each sample in a given dataset was used, in turn, as the query object, and the rest samples in the same dataset were used as the search candidates. For each query object, we compared its 100 nearest neighbors in the output space with its 100 nearest neighbors in the input space, and recorded the ratio of common neighbors in both spaces. The ratio is averaged over all query objects as the search accuracy of each algorithm. Obviously, a higher similarity search accuracy indicates a better preserving of locality structures from the input space to the output space by the algorithm.

Datasets: In the evaluation, three real datasets and five artificially generated datasets were used. The real datasets have the input representation X only; while the artificial datasets have both the input representation X and the ground-truth of the output representation Y . The datasets include:

1. GLOVE: 100- to 1000-dimensional *GloVe* word vectors [23] trained on a subset (about 330 million tokens) of wikipedia’2017 dataset² with the 50,000 most frequent English words.
2. MNIST: 784-dimensional images of handwritten digits in gray-scale [15].
3. SIFT: 128-dimensional SIFT descriptors of images used for similarity search [12].
4. ARTIFICIAL: five sets of 1,000-dimensional dense vectors (X) and 2,000-dimensional sparse binary vectors (Y). Each set corresponds to one hash length k (of 2/4/8/16/32). Each set was produced by generating 2,000-dimensional sparse binary vectors with a specific k , and then projecting the vectors to 1,000-dimensional dense vectors through principal component analysis. In this way, the samples’ pairwise distances are well preserved between the input space and the output space; i.e., $\|x_{.m} - x_{.m'}\|^2 \approx \|y_{.m} - y_{.m'}\|^2$ holds for all samples in the same set.

Algorithms to compare: We compared the proposed models with the LSH algorithm [8, 5] that maps d -dimensional inputs to k -dimensional dense vectors with a random dense projection matrix, the FLY algorithm [6] that maps d -dimensional inputs to d' -dimensional vectors with a random sparse binary projection matrix, and the LIFTING algorithm [16] that trains a sparse binary projection matrix in a supervised manner through matrix factorizations and applies the matrix for the projection (ref. Section 2.1). Both the FLY and the LIFTING algorithms also involve a WTA competition stage in the output space to get the eventual sparse binary outputs with a hash length k .

Computing environment: All the algorithms were implemented in MATLAB platform running on an 8-way server, with which 128 threads were enabled for each algorithm. For the LIFTING algorithm, IBM CPLEX was used as the linear program solver required by the Frank-Wolfe algorithm.

4.2 Supervised Training

To evaluate the supervised-WTA model, we carried out the experiments on both the artificially generated datasets and the real datasets.

On ARTIFICIAL datasets, we have both the input representation X and the output representation Y . From each dataset, we randomly chose 10,000 samples as the training set, and chose 10,000 different samples as the testing set. With the supervised-WTA model and the training samples, we trained a projection matrix W satisfying the sparse and binary constraints in Eq. (5), and projected the testing samples with the projection matrix, followed by the WTA competition to get the 2,000-dimensional sparse binary output representation. For the LIFTING algorithm, the same training and testing procedures were applied. For the LSH and the FLY algorithms, we applied them on the testing samples to get either dense or sparse binary output representations, as illustrated in Section 4.1.

For all the algorithms, we repeated the experiments for fifty runs and recorded the average accuracies. For the LSH, the FLY and the LIFTING algorithms, only the accuracies on the testing set were reported. For the supervised-WTA model, the accuracies on both the training set and the testing set were reported, denoted by SUP_{train} and SUP_{test} respectively.

From the results shown in Fig. 1(a), we can see that, consistent with the results reported in [6], the sparse binary projection algorithms reported improved results over the classical LSH method. At the same time, with the support of the supervised information, both the LIFTING algorithm and our supervised-WTA model evidently outperformed the FLY algorithm. Most prominently, with the hash length $k = 4$, the FLY algorithm has an accuracy around 8%, while the supervised-WTA model’s accuracy reaches nearly 70%. On other hash lengths, the supervised-WTA model also has significantly improved results over the FLY algorithm. When comparing the two supervised training models, the supervised-WTA model outperformed the LIFTING algorithm with all hash lengths.

In addition to the ARTIFICIAL datasets, we experimented on the GLOVE/MNIST/SIFT datasets. These real datasets only have the input representation X , but lack of the output representation Y . As suggested in [16], we computed $Y^* = \arg_Y \min \frac{1}{2} \|X^T X - Y^T Y\|_F^2 + \gamma \|Y\|_{\frac{1}{2}}$ in the feasible region of sparse binary matrices with the Frank-Wolfe algorithm, and used Y^* as the output representation that was needed by the supervised training models.

We repeated the experiments on these real datasets under the same settings. From the results shown in Fig. 1 (b-d), we can see that, again, the supervised-WTA model improved the results of the LSH and the FLY algorithms, as well as that of the LIFTING algorithm.

²<https://dumps.wikipedia.org/>

Table 1: Groups of semantically related words identified by the unsupervised-WTA model.

Groups	Words
#1	<i>me, my, our, ours, you, your, yours</i>
#2	<i>belgium, denmark, france, germany, hungary, italy, russia, switzerland</i>
#3	<i>atlantic, arctic, indian, pacific</i>
#4	<i>automobile, bicycle, car, motorcycle, truck</i>
#5	<i>africa, americas, asia, europe, oceania</i>
#6	<i>black, blue, green, purple, red, white, yellow</i>
#7	<i>mercury, venus, earth, mars, jupiter, saturn, uranus, neptune</i>
#8	<i>berkeley, caltech, cornell, harvard, mit, nyu, princeton, stanford, ucla</i>
#9	<i>adjective, adverb, noun, preposition, pronoun, verb</i>
#10	<i>astronomy, chemistry, geometry, mathematics, physics, philosophy</i>

Our next experiment investigated the influence of different input/output dimensions on the performance of the proposed models. In this experiment, we fixed the output dimension to $d' = 2,000$ while varying the input dimension from 100 to 1,000 on GLOVE word vectors. We recorded the similarity search accuracies by all algorithms. From the results shown in Fig. 2(a-d), we can see that the accuracies of all algorithms seem to have a tendency of decreasing when increasing the input dimension. While comparatively, the supervised-WTA model still reported consistently improved results under all settings.

4.3 Unsupervised Training

To evaluate the unsupervised-WTA model, we used the training samples with the input representation only to learn a projection matrix W . Then we evaluated its similarity search accuracies on both the training and the testing sets, and recorded the average performances over fifty runs. The results are denoted by UNSUP_{train} and UNSUP_{test} in Fig. 1 and Fig. 2.

The experimental results justified the effectiveness of the unsupervised-WTA model. It can be seen that the unsupervised-WTA model reported improved results over the other two unsupervised algorithms. In fact, the unsupervised-WTA model’s performance is even comparable to the supervised-WTA model, although it didn’t utilize any supervised information during the training process. Considering that data samples with the input representations are widely available in practice while the output representations may be rare, it is expected that the unsupervised-WTA model has much wider application scenarios in real situations.

As mentioned in Section 3.2, the unsupervised-WTA model can be studied from a clustering viewpoint. As a simple justification, we applied the unsupervised-WTA model on 300-dimensional GLOVE word vectors with output dimension $d' = 2,000$ and hash length $k = 4$. The generated sparse binary output vectors Y exhibited an interesting pattern. Semantically related English words were put into the same cluster which possesses the element of one in the same output dimension. As shown in Table 1, words of colors were grouped together; words of countries were grouped together; so on and so forth.

4.4 Running Speed

As a practical concern, we also measured the training time of our proposed supervised and unsupervised models, and compared them with the LIFTING algorithm. In the experiment, we used the ARTIFICIAL datasets with 1,000-dimensional inputs and 2,000-dimensional outputs, and the number of training samples varied from 1,000 to 50,000.

The running time refers to the training time needed by each algorithm to compute the sparse binary projection matrix W on each training set. Under all experimental settings, our proposed models reported significantly faster speed over the LIFTING algorithm. Fig. 3(a) shows the results of $n = 1,000$. We can see that the supervised-WTA model took only less than 0.2 seconds to get the optimal solution. It is hundreds of times faster than the LIFTING algorithm which used around 50 seconds. Comparatively, the unsupervised-WTA model needs to solve for multiple W^t and Y^t iteratively. It spent 10 to 20 seconds, which was slower than the supervised-WTA model but still

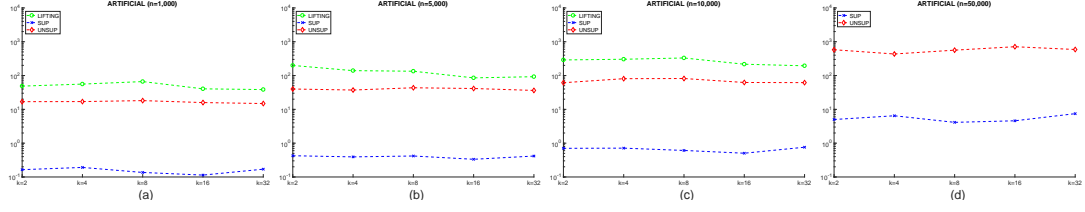


Figure 3: **Comparison of running time on GLOVE dataset with different number of samples** ($n = 1,000/5,000/10,000/50,000$). The horizontal axis is the hash length ($k = 2/4/8/16/32$). The vertical axis is the running time (seconds) in log-scale. When $n = 50,000$, the LIFTING algorithm didn't finish within 12 hours and its result is not reported. (For better visualization effect of the results shown in color, the reader is referred to the soft copy of this paper.)

several times faster than the LIFTING algorithm. In the case of $n = 50,000$ training samples shown in Fig. 3(d), the supervised-WTA model took less than 10 seconds to get the solution, and the unsupervised-WTA model took around 400 seconds. Comparatively, we didn't finish the LIFTING algorithm in our platform within 12 hours, and its time is not reported. All these real results were consistent with the complexity analysis given in Section 3.3, and justified the running efficiency of our proposed models.

5 Conclusion

With strong support from biological science, the study of sparse binary projection models has attracted much research attention recently. Through converting lower-dimensional dense data to higher-dimensional sparse binary vectors, the models have achieved excellent empirical results and provided a useful tool in practical applications.

Biologically, the winner-take-all competition is an important stage for pattern recognition activities that happen in the brain. Our work started from the modeling of the WTA competition, and proposed two models to seek the desired projection matrix for sparse binary projections. The supervised-WTA model utilizes both input and output representations of the samples, and trains the projection matrix as a supervised learning problem. The unsupervised-WTA model requires the input representation only, which equips the model with wider application scenarios. For the models, we have developed simple, efficient and effective algorithms. In the evaluation on similarity search tasks, our models significantly outperformed the state-of-the-art methods, in both search accuracy and running time.

Our work potentially triggers a number of topics for future study. Firstly, as mentioned in Section 3.3, the algorithms for both models only involve simple vector addition and scalar comparison operations, which are highly parallelizable. Such characteristics make the computing procedures very suitable to be implemented with customized hardware such as in the FPGA platform [20], which will provide a high-throughput and economical solution for large scale data analysis applications.

Secondly, as mentioned in Section 3.2, the unsupervised-WTA model has a natural relationship with the clustering and the feature selection models. It provides a unified framework that combines these two techniques. We believe that investigating new clustering and feature selection applications following this viewpoint is possible. More importantly, we believe that clustering and feature selection may be a potential bridge that helps to make clear why modeling the WTA competition could lead to algorithms that preserve the locality structures of the data well, as reported in this paper.

The third potential is in designing new artificial neural network architectures. The approach we adopted in this paper can be potentially used as an activation function of the neurons in an artificial neural network. We highly anticipate future research work along this line [22, 17].

Acknowledgements

This work was supported by Shenzhen Fundamental Research Fund (JCYJ20170306141038939, KQJSCX20170728162302784).

References

- [1] M. Arbib. *The Handbook of Brain Theory and Neural Networks*. MIT Press, 2003.
- [2] R. Baeza-Yates and B. Ribeiro-Neto. *Modern Information Retrieval*, volume 463. ACM Press, 1999.
- [3] E. Bingham and H. Mannila. Random projection in dimensionality reduction: applications to image and text data. In *Proceedings of the 7th ACM SIGKDD International Conference on Knowledge Discovery and Data Mining*, pages 245–250. ACM, 2001.
- [4] S. Caron, V. Ruta, L. Abbott, and R. Axel. Random convergence of olfactory inputs in the drosophila mushroom body. *Nature*, 497(7447):113, 2013.
- [5] M. Charikar. Similarity estimation techniques from rounding algorithms. In *Proceedings of the 34th Annual ACM Symposium on Theory of Computing*, pages 380–388. ACM, 2002.
- [6] S. Dasgupta, C. Stevens, and S. Navlakha. A neural algorithm for a fundamental computing problem. *Science*, 358(6364):793–796, 2017.
- [7] M. Frank and P. Wolfe. An algorithm for quadratic programming. *Naval Research Logistics*, 3(1-2):95–110, 1956.
- [8] A. Gionis, P. Indyk, and R. Motwani. Similarity search in high dimensions via hashing. In *Proceedings of 25th International Conference on Very Large Data Bases*, volume 99, pages 518–529, 1999.
- [9] I. Guyon and A. Elisseeff. An introduction to variable and feature selection. *Journal of Machine Learning Research*, 3(Mar):1157–1182, 2003.
- [10] M. Jaggi. Revisiting Frank-Wolfe: Projection-free sparse convex optimization. In *Proceedings of the 30th International Conference on Machine Learning*, pages 427–435, 2013.
- [11] A. Jain, N. Murty, and P. Flynn. Data clustering: a review. *ACM Computing Surveys*, 31(3):264–323, 1999.
- [12] H. Jegou, M. Douze, and C. Schmid. Product quantization for nearest neighbor search. *IEEE Transactions on Pattern Analysis and Machine Intelligence*, 33(1):117–128, 2011.
- [13] W. Johnson and J. Lindenstrauss. Extensions of Lipschitz mappings into a Hilbert space. *Contemporary Mathematics*, 26(189-206):1, 1984.
- [14] T. Kohonen. The self-organizing map. *Proceedings of the IEEE*, 78(9):1464–1480, 1990.
- [15] Y. LeCun, L. Bottou, Y. Bengio, and P. Haffner. Gradient-based learning applied to document recognition. *Proceedings of the IEEE*, 86(11):2278–2324, 1998.
- [16] W. Li, J. Mao, Y. Zhang, and S. Cui. Fast similarity search via optimal sparse lifting. In *Advances in Neural Information Processing Systems*, pages 176–184, 2018.
- [17] N. Lynch, C. Musco, and M. Parter. Winner-take-all computation in spiking neural networks. *arXiv preprint arXiv:1904.12591*, 2019.
- [18] W. Maass. On the computational power of winner-take-all. *Neural computation*, 12(11):2519–2535, 2000.
- [19] S. Olsen, V. Bhandawat, and R. Wilson. Divisive normalization in olfactory population codes. *Neuron*, 66(2):287–299, 2010.
- [20] A. Omondi and J. Rajapakse. *FPGA Implementations of Neural Networks*, volume 365. Springer, 2006.
- [21] K. Panousis, S. Chatzis, and S. Theodoridis. Nonparametric bayesian deep networks with local competition. In *Proceedings of the 36th International Conference on Machine Learning*, 2019.
- [22] C. Pehlevan, A. Sengupta, and D. Chklovskii. Why do similarity matching objectives lead to hebbian/anti-hebbian networks? *Neural Computation*, 30(1):84–124, 2018.
- [23] J. Pennington, R. Socher, and C. Manning. Glove: Global vectors for word representation. In *Proceedings of the 2014 Conference on Empirical Methods in Natural Language Processing*, pages 1532–1543, 2014.
- [24] C. Stevens. What the fly’s nose tells the fly’s brain. *Proceedings of the National Academy of Sciences*, 112(30):9460–9465, 2015.
- [25] G. Turner, M. Bazhenov, and G. Laurent. Olfactory representations by drosophila mushroom body neurons. *Journal of Neurophysiology*, 99(2):734–746, 2008.
- [26] Z. Zheng, S. Lauritzen, E. Perlman, C. Robinson, et al. A complete electron microscopy volume of the brain of adult drosophila melanogaster. *Cell*, 174(3):730–743, 2018.